At Shell Polymers, we're dedicated to helping our customers create a stronger polyethylene supply chain. That's why we're reimagining the polyethylene industry with our state-of-the-art plant technologies and trusted, tested industry experts. This commitment to offering an unrivaled customer experience by streamlining your supply chain is just one way we **Break the Mold.**

SHELL POLYMERS
MAKING THE EXPERIENCE MATTER

Click here to learn more about Shell Polymers

Received: 22 June 2020 | Revised: 16 July 2020 | Accepted: 18 July 2020

DOI: 10.1002/pol.20200436

ORIGINAL ARTICLE

JOURNAL OF POLYMER SCIENCE WILEY

Chain-growth polycondensation via the substituent effect: Investigation in to the role of initiator and base on the synthesis of poly(*N*-octyl benzamide)

Frederick C. Prehn Jr[1] | **Brian D. Etz**[1] | **Daniel Price**[2] | **Amanda Trainor**[3] | **Caleb J. Reese**[4] | **Shubham Vyas**[1] | **Stephen G. Boyes**[4]

[1]Department of Chemistry, Colorado School of Mines, Golden, Colorado

[2]Science Department, Columbine High School, Littleton, Colorado

[3]Department of Chemistry, Saint Michael's College, Colchester, Vermont

[4]Department of Chemistry, The George Washington University, Washington, District of Columbia

Correspondence
Stephen G. Boyes, Department of Chemistry, The George Washington University, Washington, DC 20052.
Email: sboyes@gwu.edu

Funding information
National Science Foundation, Grant/Award Numbers: CHE MSN #1807863, ENG #1460712

Abstract

A detailed investigation into the role of initiator structure, the presence of an initiator, and basicity of the non-nucleophilic base in the chain-growth condensation (CGC) synthesis of poly(*N*-octyl benzamide) was conducted. A series of phenyl ester dimethyl amide initiators with different leaving groups were synthesized and used in the CGC preparation of poly(*N*-octyl benzamide). Additional polymerizations were conducted without the presence of an initiator and with different non-nucleophilic bases. Kinetic studies, along with nuclear magnetic resonance spectroscopy and gel-permeation chromatography, were used to determine progress of the reaction, molecular weights, and molecular weight distributions. The experimental and computational results demonstrated that initiators containing electron-withdrawing substituent phenyl esters, such as the p-nitrophenyl ester, and electron-withdrawing carbonyl character on the parent benzoate produce polymers with controllable molecular weights and narrow molecular weight distributions. Whereas, initiating species that contain electron-donating character on the benzoate backbone, such as dimethylamino and methyl ester groups, produce polymers that resemble the results from reactions involving no initiators at all, indicating poor polymerization control.

KEYWORDS

aromatic polyamides, chain-growth condensation, initiator, non-nucleophilic bases, substituent effects

1 | INTRODUCTION

Chain-growth condensation (CGC) polymers are a relatively new class of polymers that have allowed for the preparation of traditional step-growth polymers with new functionalities, while also providing control over molecular weight and end group chemistries and producing polymers with narrow molecular weight distributions.[1] These improvements provide the opportunity for the preparation of materials that have historically, not been possible using traditional step-growth methods. One such example is aromatic polyamides. Using the CGC process, aromatic polyamides with controlled molecular weight, narrow molecular weight distributions, and complex architecture, including block, hyperbranched, star, and comb copolymers, have been synthesized.[2]

The theory behind the CGC process has been extensively reviewed by Yokozawa and coworkers.[1–6] The

main concept behind the CGC preparation of aromatic polyamides involves nucleophilic acyl substitution at the ester substituent end group of the growing chain. The literature proposes that control over the polymerization is achieved when the reactivity of the ester substituent on the monomer is much less than the reactivity of the ester on an initiator or the growing chain, causing polymer growth to occur only at the chain end, after initiation.[3] It is argued that the decrease in reactivity of the monomer's ester group is obtained when the deprotonated amine donates negative charge into the ring, deactivating the para ester substituent. This deactivation is explained by a decrease in the electrophilicity of the carbonyl carbon from the shielding nature of the electron-rich ring.

It is well understood in more conventional controlled polymerization techniques, such as living radical polymerizations, that control over molecular weight and narrow molecular weight distributions occur when initiation is fast relative to propagation, in addition to reducing termination processes.[7] This also applies to CGC systems when attempting to obtain optimum control over the polymerization. As such, it is evident that an initiator with an ester group that is more reactive than the propagating polymer chain is required to produce well-defined polymers via the CGC process. This concept was particularly evident in the recent work from our group that examined the effect of monomer structure on the kinetics of CGC polymerization in the preparation of poly(*N*-octyl benzamide)[8] This work demonstrated that the reactivity of substituted phenyl 4-octylaminobenzoate monomers dramatically increased, when the monomer contained an electron-withdrawing phenyl ester group as the leaving group in the nucleophilic acyl substitution reaction to add monomer to the polymer chain end. However, when polymerizing these reactive monomers, it was observed that control over the polymerization was decreased when using conventional initiators for CGC systems. This loss of control was attributed to competition between the conventionally accepted initiation mechanism for CGC and a self-initiation process due to the enhanced reactivity of the monomer.

As such, a thorough understanding of the initiation process and factors influencing the self-initiation process is critical. Despite this, the reactivity of deprotonated monomer in solution with itself has received little attention, with only one study where self-initiation was investigated by employing a premade self-condensed dimer as an initiator using the CsF activation method.[9] Results of this study show that dimers do behave like initiators (or growing polymer chains) due to the amide linkage between the monomers not reducing the reactivity of the ester group despite the presence of a deprotonated amine. Therefore, this process could be a plausible mechanism for describing the self-initiation observed when using very reactive monomers.

This study investigates how monomers with more reactive ester substituents do not follow the accepted theory for monomer deactivation in the CGC process. To examine this, three substituted phenyl 4-octylaminobenzoate monomers, with different ester-leaving groups, were synthesized and exposed to CGC polymerization conditions without the addition of an initiator. In addition, a series of initiators with different ester-leaving groups were also synthesized to investigate the effect of the initiator activity on control over the polymerization and the role of the basicity of the non-nucleophilic base on the initiation process was also studied.

2 | EXPERIMENTAL

2.1 | Materials

Lithium 1,1,1,3,3,3-hexamethyldisilazide (LiHMDS, 1.0 M) in tetrahydrofuran (THF), lithium diisopropylamide (LDA, 1.0 M, THF), dimethylamine solution (2 M, THF), triethylamine (>99.5%), thionyl chloride ($SOCl_2$, >99.5%), anhydrous dichloromethane (DCM) (stabilized with 50–150 ppm amylene, >99.8%), octanal (99%), sodium triacetoxyborohydride (97%), 4-(dimethylcarbamoyl)benzoic acid (98%), 4-nitrophenol (99%), p-toluic acid (98%), dimethylformamide (DMF, anhydrous, 99.8%) and $MgSO_4$ were purchased from Sigma Aldrich. Acetic acid, sodium bicarbonate, sodium hydroxide, and ethyl acetate were purchased from Macron. Ammonium chloride (99.9%) was purchased from Baker Scientific and methyl 4-aminobenzoate (98%) from Alfa Aesar. 4-*N*,*N*-dimethylaminopyridine (DMAP, 99%), and dicyclohexylcarbodiimide (DCC, 99%) were purchased from Acros Organics. 4-Methylphenol was purchased from Fluka Analytical. Unless otherwise mentioned, all chemicals were used as received without further purification. THF was purchased from Macron and was purified and dispensed through a PURE SOLV MD-4 solvent purification system (activated alumina, copper catalysts, and molecular sieves).

2.2 | Instruments and characterization

^{1}H, ^{13}C, and ^{19}F nuclear magnetic resonance (NMR) spectra were obtained on a JEOL-500 S MHz spectrometer. Infrared spectra were recorded on a Thermo Scientific Nicolet iS50 Fourier transform infrared (FTIR) spectrometer using a diamond attenuated total reflectance (ATR) crystal. Number-average molecular weight (M_n) and polydispersity index (M_w/M_n, PDI) were

measured using a Viscotek GPCmax gel-permeation chromatography (GPC) unit (eluent: stabilized tetrahydrofuran (OmniSolv) with a flow rate of 1.0 ml/min using PLgel 5 μm MIXED-C and MIXED-D columns: molecular weight range 200–2,000,000 and 200–400,000 g/mol (polystyrene equivalent), respectively). A calculated d*n*/d*c* value of 0.156 was determined and used during the molecular weight analysis.

2.3 | Synthesis of N-octyl monomers

The procedure for N-alkylation of the various 4-aminobenzoate esters was adapted from the literature.[10] To reduce the length of the paper, the experimental details of the for synthesis of the 4-aminobenzoate precursors is included in the supporting information.

2.3.1 | Methyl 4-(octylamino)benzoate (M-OAB)

Methyl 4-aminobenzoate (6.0 g, 38.9 mmol), octanal (5 g, 38.9 mmol), acetic acid (2.9 ml, 51.3 mmol), and sodium triacetoxy- borohydride (9.89 g, 46.7 mmol). Product: as white crystals; mp 89–90°C, (8.3 g, yield 81%). ^{1}H NMR (500 MHz, $CDCl_3$, δ): 7.85 (d, J = 8.9 Hz, 2H, ArH), 6.54 (d, J = 8.9 Hz, 2H, ArH), 4.13 (br, 1H), 3.83 (s, 3H), 3.14 (t, J = 7.4 Hz, 2H), 1.62 (q, J = 7.4 Hz, 2H), 1.42–1.22 (m, 10H), 0.88 (t, J = 7.4 Hz, 3H). ^{13}C NMR (125 MHz, $CDCl_3$, δ): 167.3, 152.1, 131.4, 117.6, 111.1, 51.3, 43.2, 31.7, 29.2, 29.16, 29.1, 27.0, 22.5, 14.0.; FTIR (ATR): ν = 3,376 (Ar—NH—R), 2,946, 2,920, 2,849 (C—H), 1,678 (O—C═O), 1,596, 1,430, 1,190, 1,105, and 832 cm^{-1}.

2.3.2 | Phenyl 4-(octylamino)benzoate (P-OAB)

Phenyl 4-aminobenzoate (6.0 g, 28.3 mmol), octanal (3.62 g, 28.3 mmol), acetic acid (2.4 ml, 42.4 mmol), and sodium triacetoxy-borohydride (7.8 g, 36.8 mmol). Product: as white crystals; mp 112–113°C, (7.3 g, yield 79%). ^{1}H NMR (500 MHz, $CDCl_3$, δ): 8.0 (d, J = 8.9 Hz, 2H, ArH), 7.4 (t, J = 8.1 Hz, 2H, ArH), 7.25 (t, J = 8.1 Hz, 1H, ArH), 7.18 (d, J = 8.1 Hz, 2H, ArH), 6.59 (d, J = 8.9 Hz, 2H, ArH), 4.2 (br, 1H), 3.2 (t, J = 7.4 Hz, 2H), 1.6 (q, J = 7.4 Hz, 2H), 1.42–1.22 (m, 10H), 0.88 (t, J = 7.4 Hz, 3H). ^{13}C NMR (125 MHz, $CDCl_3$, δ): 167.3, 152.1, 131.4, 117.6, 111.1, 51.3, 43.2, 31.7, 29.2, 29.16, 29.1, 27.0, 22.5, 14.0.; FTIR (ATR): ν = 3,380 (Ar—NH—R), 2,921, 2,852 (C—H), 1,691 (O—C═O), 1,594, 1,275, 1,163, 1,075, 742 cm^{-1}.

2.3.3 | Trifluoromethylphenyl 4-(octylamino)benzoate (TFMP-OAB)

Trifluoromethylphenyl 4-aminobenzoate (5.0 g, 17.8 mmol), octanal (2.3 g, 17.8 mmol), acetic acid (1.5 mL, 26.7 mmol), and sodium triacetoxyborohydride (4.9 g, 23.1 mmol). Product: as white crystals; mp 129–130°C, (4.9 g, yield 70%). ^{1}H NMR (500 MHz, $CDCl_3$, δ): 8.0 (d, J = 8.9 Hz, 2H, ArH), 7.7 (d, J = 8.9 Hz, 2H, ArH), 7.3 (d, J = 8.9 Hz, 2H, ArH), 6.59 (d, J = 8.9 Hz, 2H, ArH), 4.25 (br, 1H), 3.2 (t, J = 7.4 Hz, 2H), 1.6 (q, J = 7.4 Hz, 2H), 1.42–1.22 (m, 10H), 0.88 (t, J = 7.4 Hz, 3H). ^{13}C NMR (125 MHz, $CDCl_3$, δ): 164.9, 152.9, 132.5, 126.7 (q, J = 3.8 Hz) (C—F), 122.5, 116.2, 111.5, 43.2, 31.7, 29.2, 29.16, 29.1, 27.0, 22.5, 14.0. ^{19}F NMR 1 peak; FTIR (ATR): ν = 3,376 (Ar-NH-R), 2,952, 2,924, 2,854 (C—H), 1,698 (O—C═O), 1,598, 1,320, 1,272, 1,159, 1,120, 1,058, 833, and 761 cm^{-1}.

2.4 | Synthesis of substituted initiators

2.4.1 | Methyl 4-(dimethylcarbamoyl) benzoate (DMA-M)

A solution of dimethylamine (4 ml, 8 mmol), triethylamine (0.87 ml, 6.3 mmol), and anhydrous DCM (15 ml) was prepared and added to a solution of the acid chloride (methyl 4- (chlorocarbonyl)benzoate) (1.13 g, 5.7 mmol) (prepared by refluxing 4-(methoxycarbonyl) benzoic acid (1.03 g, 5.7 mmol) in $SOCl_2$ for 2 hr, and removing excess $SOCl_2$) in anhydrous DCM (5 ml). The solution was refluxed for 1 hr followed by concentration in vacuo. The crude reaction mixture was purified by flash column chromatography on silica gel (pentane/ethyl acetate 1:1). Product: off yellow solid. mp 108–109°C, (1.1 g, yield: 91%). ^{1}H NMR (500 MHz, $CDCl_3$, 25°C): δ = 8.06 (d, J = 8.32 Hz, 2H), 7.47 (d, J = 8.32 Hz, 2H), 3.92 (s, 3H), 3.11 (br, 3H), 2.94 (br, 3H); ^{13}C NMR (125 MHz, $CDCl_3$) 170.5, 166.5, 140.7, 131.0, 129.7, 127.2, 52.4, 39.4, 35.3 ppm; FTIR (ATR): 2951, 2,853, 1721, 1,618, 1,277, 1,257, 1,109, 1,078, and 726 cm^{-1}.

2.4.2 | Phenyl 4-(dimethylcarbamoyl) benzoate (DMA-P)

DMA-P is synthesized using a previously reported procedure with the following conditions[8]: 4-(phenoxycarbonyl) benzoic acid (1.1 g, 4.5 mmol), $SOCl_2$ (11 ml, 150 mmol), dimethylamine (2.73 ml, 5.5 mmol), triethylamine (0.7 ml, 5.0 mmol), and DCM (20 ml). Product: as white crystals; mp 111–112°C, (0.86 g, yield 70%).^{1}H NMR (500 MHz,

$CDCl_3$, δ): 8.2 (d, $J = 8.1$ Hz, 2H, ArH), 7.54 (d, $J = 8.2$ Hz, 2H, ArH), 7.42 (t, $J = 8.0$ Hz, 2H, Ar H), 7.27 (t, $J = 8.0$ Hz, 1H, ArH), 7.21 (d, $J = 8.0$ Hz, 2H, ArH), 3.1, (s, 3H) 2.97 (s, 3H) (N—CH_3); ^{13}C NMR (150 MHz, $CDCl_3$, δ): 170.5, 164.6, 150.9, 141.4, 130.46, 130.40, 129.6, 127.3, 126.1, 121.7, 39.4, 35.4; FTIR (ATR): ν = 3,085, 2,920, 1,724 (O—C═O), 1,616 (N—C═O), 1,393, 1,265, 1,085, 876, 720 cm^{-1}.

A different synthesis scheme was used for the synthesis of the substituted phenyl ester dimethyl amide initiators (Scheme 1). The synthesis scheme and detailed procedures for the precursors can be found in the supplementary information. The following is a representative procedure for the coupling of the benzoic acid precursor and substituted phenol.

2.4.3 | 4-Nitrophenyl 4-(dimethylcarbamoyl)benzoate (DMA-NP)

4-(Dimethylcarbamoyl) benzoic acid (1.63 g, 8.44 mmol) was added to anhydrous DMF (40 ml) in a round-bottom flask equipped with a stir bar. 4-Nitrophenol (1.17 g, 8.44 mmol) and DMAP (0.060 g, 0.5 mmol) were then added and stirred to dissolve. DCC (1.74 g, 8.44 mmol) was added slowly to the reaction mixture. The resulting solution was allowed to stir overnight. The urea by-product was removed using vacuum filtration and solvent was then removed under vacuum. The resulting paste was then dissolved in chloroform and passed through a silica column. The solvent was removed, and the resulting product was recrystallized from methanol. Product: as white crystals; mp 166–167°C, (1.78 g, yield 67%).^{1}H NMR (500 MHz, $CDCl_3$, δ): 8.32 (d, $J = 8.1$ Hz, 2H, ArH), 8.23 (d, $J = 8.1$ Hz, 2H, ArH), 7.57 (d, $J = 8.0$ Hz, 2H, ArH), 7.42 (d, $J = 8.0$ Hz, 2H, ArH), 3.1, (s, 3H) 2.97 (s, 3H) (N—CH_3); ^{13}C NMR (150 MHz, $CDCl_3$, δ): 170.2, 163.6, 155.5, 145.6, 142.1, 130.6, 129.4, 127.5, 125.4, 122.7, 39.48, 35.4; FTIR (ATR): ν = 3,064, 2,930, 1731 (O—C═O), 1,610 (N—C═O), 1,522, 1,397, 1,211, 1,085, 887, 737 cm^{-1}.

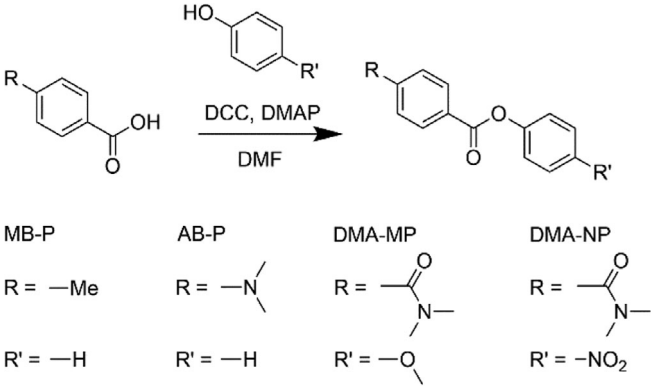

SCHEME 1 Synthesis of functionalized phenyl ester dimethyl amide initiator using DCC/DMAP

2.4.4 | 4-Methoxyphenyl 4-(dimethylcarbamoyl)benzoate (DMA-MP)

4-(Dimethylcarbamoyl) benzoic acid (2.03 g, 10.51 mmol), DMF (50 ml), 4-methoxyphenol (1.31 g, 10.51 mmol), DMAP (0.060 g, 0.5 mmol), and DCC (2.17 g, 10.51 mmol). Product: as white crystals; mp 131–132°C, (2.43 g, yield 77%). ^{1}H NMR (500 MHz, $CDCl_3$, δ): 8.2 (d, $J = 8.1$ Hz, 2H, ArH), 7.54 (d, $J = 8.2$ Hz, 2H, ArH), 7.12 (d, $J = 8.1$ Hz, 2H, Ar H), 6.95 (d, $J = 8.1$ Hz, 2H, ArH), 3.65, (s, 3H) 3.16 (s, 3H), 2.95 (s, 3H, N—CH_3); ^{13}C NMR (150 MHz, $CDCl_3$, δ): 170.5, 165.0, 150.9, 157.5, 144.3, 141.3, 130.6, 130.3, 127.2, 122.5, 114.6, 55.7, 35.4; FTIR (ATR): ν = 2,834, 1,728 (O—C═O), 1,620 (N—C═O), 1,620, 1,504, 1,392, 1,262, 1,201, 1,071, 1,034, 1,071, 737, 662, 528 cm^{-1}.

2.4.5 | Phenyl 4-(dimethylamino) benzoate (AB-P)

4-(Dimethylamino) benzoic acid (3.0 g, 18.16 mmol), DMF (40 ml), phenol (1.71 g, 18.16 mmol), DMAP (0.11 g, 0.91 mmol), and DCC (3.75 g, 18.16 mmol). Product: as white crystals; mp 178–179°C, (2.88 g, yield 67%).^{1}H NMR (500 MHz, $CDCl_3$, δ): 8.06 (d, $J = 8.1$ Hz, 2H, ArH), 7.40 (t, $J = 8.1$ Hz, 2H, ArH), 7.23 (t, $J = 8.0$ Hz, 1H, ArH), 7.19 (d, $J = 8.0$ Hz, 2H, ArH), 3.08, (s, 6H); ^{13}C NMR (150 MHz, $CDCl_3$, δ): 165.7, 153.7, 151.3, 132.1, 129.4, 125.5, 122.1, 116.1, 110.8, 40.2; FTIR (ATR): ν = 2,930, 1,705 (O—C═O), 1,594, 1,368, 1,275, 1,066, 825, 760, 696, 486 cm^{-1}.

2.4.6 | Phenyl 4-methylbenzoate (MB-P)

p-Toluic acid (1.36 g, 10.0 mmol), DMF (40 ml), phenol (0.94 g, 10.0 mmol), DMAP (0.10 g, 0.94 mmol), and DCC (2.06 g, 10 mmol). Product: as white crystals; mp 74–75°C, (1.67 g, yield 78%).^{1}H NMR (500 MHz, $CDCl_3$, δ): 8.09 (d, $J = 8.3$ Hz, 2H, ArH), 7.42 (t, $J = 8.2$ Hz, 2H, ArH), 7.31 (d, $J = 8.2$ Hz, 2H, ArH), 7.26 (t, $J = 8.1$ Hz, 1H, ArH), 7.2 (d, $J = 8.2$ Hz, 2H, ArH), 2.45 (s, 3H); ^{13}C NMR (150 MHz, $CDCl_3$, δ): 165.3, 151.1, 144.4, 130.3, 129.5, 129.4, 126.9, 125.8, 121.9, 21.9; FTIR (ATR): ν = 3,308, 2,924, 2,850, 1,720 (O—C═O), 1,268, 1,190, 1,079, 743, 686 cm^{-1}.

2.5 | Polymerization methods

2.5.1 | Polymerization employing no initiator and LiHMDS Base

A typical polymerization procedure where no initiator was used is depicted in Scheme 2. The reaction was conducted by placing 0.5 mmol of a given monomer (0.13 g M-OAB, 0.162 g P-OAB, or 0.195 g TFMP-OAB) in a 25 ml round-bottom flask with a stir bar. The flask was then capped with a septum and purged with argon. Anhydrous THF (10 ml for 1 equivalent of base experiments or 5 ml for 10 equivalents of base) was then injected into the flask containing the monomer, and the solution was brought to the temperature of interest using a cooling bath. LiHMDS (0.6 ml, 0.6 mmol for one equivalent of base or 5 ml, 5 mmol for 10 equivalents of base) was then injected to start the polymerization. Aliquots were removed and quenched, by injecting into a saturated ammonium chloride solution, during the course of the polymerization. The resulting polymer was isolated via extraction with DCM, washed with aqueous 1 M NaOH, dried using magnesium sulfate, and isolated by removing the solvent under vacuum, followed by further drying in a vacuum oven at 60°C for 2 hr.

Due to the high reactivity of the trifluoromethylphenyl monomer, the two temperatures of interest were −48°C (achieved using dry ice and acetonitrile) and −20°C (brine ice bath). The lower reactivity of the phenyl and methyl moiety resulted in the experiments being conducted at −20 and 0°C (conventional ice bath).

2.5.2 | Polymerizations employing LDA base

A typical polymerization procedure using the MB-P initiator, the monomer of interest, and LDA as the base is depicted in Scheme S1. The reactions were conducted by adding 0.5 mmol of a given monomer (0.13 g M-OAB, 0.162 g P-OAB, 0.195 g TFMP-OAB) and the initiator, phenyl 4-methylbenzoate (MB-P) (0.0021 g, 0.01 mmol), in a 25 ml round-bottom flask equipped with a stir bar. The flask was capped with a septum and then purged with argon. Anhydrous THF (10 ml) was injected into the flask and the solution was brought to −20°C. LDA (0.5 ml, 0.5 mmol), was then injected into the solution to start the polymerization. The reaction containing the methyl ester monomer (M-OAB) was warmed to room temperature (20°C) after addition of the LDA, while for the remaining monomers (P-OAB and TFMP-OAB) the reaction was kept at −20°C. After 6 hr, the solution was then poured into a saturated ammonium chloride solution. The resulting polymer was isolated via extraction with DCM, washed with aqueous 1 M NaOH, dried using magnesium sulfate, and isolated by removing the solvent under vacuum, followed by further drying in a vacuum oven at 60°C for 2 hr.

2.5.3 | Polymerization employing various initiators

A typical polymerization procedure using the desired initiator and the monomer of interest is depicted in Scheme 3. A volume of 0.5 mmol of a given monomer (0.13 g M-OAB, 0.162 g P-OAB, 0.195 g TFMP-OAB) and 0.01 mmol of the desired initiator (2.4 mg AB-P, 2.1 mg MB-P, 3.1 mg DMA-NP, 3.0 mg DMA-MP, 10.4 mg DMA-M, 2.7 mg DMA-P) was added to a 25 ml

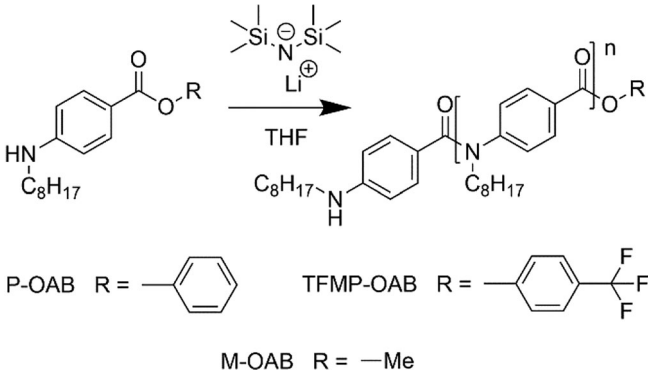

SCHEME 2 Self-initiation polymerization reaction, where the monomer reacts without initiator to produce polymer

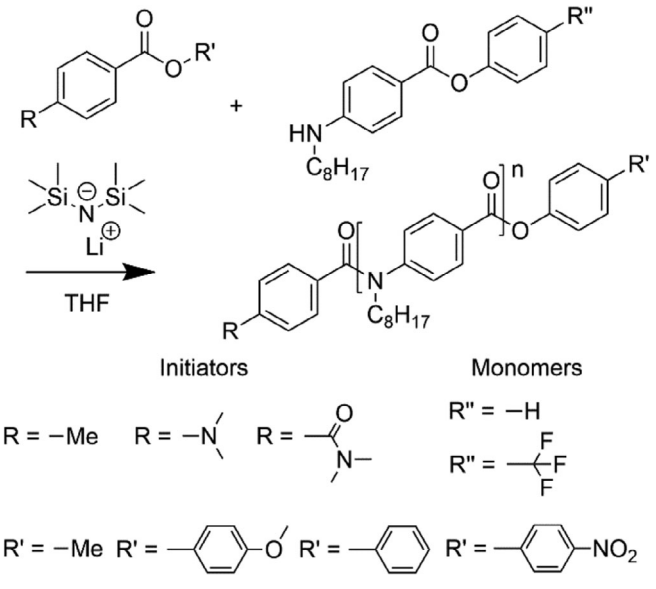

SCHEME 3 Polymerization scheme employing initiators with varying reactivity

round-bottom flask equipped with a stir bar. The flask was capped with a septum and then purged with argon. Anhydrous THF (10 ml) was injected into the flask and the solution was brought the temperature of interest using a cooling bath. LiHMDS (0.6 ml, 0.6 mmol) was injected into the solution to start the polymerization. After 2 hr, the solution was poured into a saturated ammonium chloride solution. The resulting polymer was isolated via extraction with dichloromethane, washed with aqueous 1 M NaOH, dried using magnesium sulfate, and isolated by removing the solvent under vacuum, followed by further drying in a vacuum oven at 60°C for 2 hr.

2.6 | Computation modeling parameters

All computations used the high-performance computing facility accessible through the Colorado School of Mines. The Gaussian 09 package was used for all calculations performed during this study.[11] Geometry and transition state optimizations were performed using the 2006 version of the Global hybrid Minnesota functional (M06-2X)[12] and the split valance polarized basis set 6-31G(d).[13,14] The transition states were confirmed with frequency calculations, with the force constants computed at the first point and with suppression of the Eigen test. The charge of each atom was calculated using a natural bond orbital analysis.[15] Implicit solvation of THF was incorporated into the calculations using the integral equation formalism variant polarizable continuum mode.[16] HOMO and LUMO plots were generated on the basis of calculating the areas of electron density at the highest occupied and lowest unoccupied molecular orbitals. Activation energies and reaction rates for the polymer growth mechanism were gained from implementing the KisThelP package.[17]

3 | RESULTS AND DISCUSSION

The CGC process has allowed for the synthesis of polymers, typically prepared using conventional step-growth polymerization, with controlled molecular weights, narrow molecular weight distributions, improved functionality, and more complex architectures.[2] Previous work has demonstrated that well-defined aromatic polyamides can be produced using the CGC method with various phenyl 4-octylaminobenzoate monomers, a strong non-nucleophilic lithium amide base to prepare the amide anion on the monomer, and an initiating species containing an activated ester.[8,18,19] Within this work, there has been a preference toward methyl ester-based monomers for CGC, as these monomers yield low-boiling point methanol as the by-product after the aqueous workup, which is claimed to make the overall process more convenient.[10] However, previous work by our group using the methyl ester monomer M-OAB to produce polymer brushes from surface-immobilized initiators, demonstrated that even though polymer brushes could be formed, issues with by-product solubility and slow kinetics restricted the thickness of the polymer brushes.[20] In an effort to better understand the effect of monomer structure on the kinetics of the CGC process and on the polymers produced, we recently investigated the polymerization of a variety of N-octyl benzamide-based monomers with different ester substituents.[8] The main conclusion from this work was that the structure of the monomers ester-leaving group dictates the reactivity of the monomer in CGC and the solubility of the polymerization by-products. One of the most interesting observations from this previous study was that, while the phenyl ester monomers demonstrated faster reactivity and increased solubility of the lithium phenoxide by-products, they were also more difficult to control during polymerization, which resulted in broader molecular weight distributions and multimodal GPC traces. This loss of control was attributed to the competition between the conventionally accepted initiation mechanism for CGC and a self-initiation process due to the enhanced reactivity of the monomer. Despite the dramatic effect self-initiation can have on control of the CGC process, to the best of our knowledge, there is only one previous paper that considers self-initiation in detail.[9] However, that paper only investigates dimer-based initiation in a system with CsF activation, which is not commonly used.

3.1 | Effect of no initiator and different molar equivalent of LiHMDS to monomer on CGC

To better understand the self-initiation process in CGC, three different N-octyl benzamide-based monomers, with different ester substituents and of varying activity, were synthesized and, subsequently, polymerized without the presence of initiator and with different molar equivalents of the base LiHMDS (Scheme 2). The methyl ester monomer M-OAB was chosen as a control, since it has been extensively used in previous studies.[8,18,20–24] The polymerization of M-OAB with no initiator and 1 M equivalent of LiHMDS yielded no measurable polymer formation over a 12 hr period at either 0 or −20°C, indicating that, at these temperatures, self-initiation is not present for the commonly used M-OAB monomer. However, our previous studies have demonstrated that the

methyl ester monomer has low reactivity at these temperatures, even in the presence of initiator, due to the basicity of the methoxide-leaving group.[8]

Next, the self-initiation properties of the two more reactive monomers, P-OAB and TFMP-OAB, at 0 and −20°C with no initiator added was investigated. Results from these experiments show that in each case, polymer forms when no initiator is employed. The molecular weight evolution with time from a typical polymerization for P-OAB with no initiator at 0°C and TFMP-OAB with no initiator at −20°C is shown in Figure 1. From these GPC traces, it is clear that the monomer signal, near a retention volume of 18.5 ml, decreases with time, while the polymer signal moves left, indicating an increasing molecular weight. However, along with the increasing molecular weight, there is also a broadening of the molecular weight distribution. In addition, the GPC traces for polymerization of the faster TFMP-OAB monomer show a multimodal peak, which suggests that polymer chains are being initiated at various stages during the polymerization. These results demonstrate that self-initiation not only takes place in the systems with the more reactive P-OAB and TFMP-OAB monomers, but it is also occurring over the course of the reaction, resulting in increased PDIs. These observations were also confirmed in plots of molecular weight and PDI versus monomer conversion (Figure 2). The NMR conversion data was obtained using the ratio of the monomer doublet signal to the broader polymer doublet signal of the aryl protons adjacent to the substituted aniline group. Figure 2 shows that in each case the molecular weight increases with conversion. The PDI values were consistently higher than the systems where initiator was used and, in general, tended to increase with conversion for the systems without initiator.

To further investigate self-initiation, the kinetics of the polymerization of both P-OAB and TFMP-OAB were followed by semilogarithmic plots of conversion versus time at various temperatures, base concentrations, and with and without added initiator (Figure 3). These plots show that in most cases there is a linear relationship; however, the slope of the plots, at a given temperature for a given monomer differs showing different rates of reaction. As a constant concentration of monomer was used in each case, the varying rates, at a particular temperature, are due to different concentrations of active chains, which is presumably as a result of different concentrations of initiating species. In each case, the polymerizations generally followed first-order kinetics, which is characteristic of a CGC polymerization. If the polymerization followed a step-growth mechanism, these plots would not be linear due to different kinetic expressions resulting from the step-growth process. It is evident that the use of an initiator increases the rate and maintains control over the reaction. It is also apparent that for the polymerizations without addition of an initiator, polymer still forms, and the polymerizations generally follows first-order kinetics. These results further suggest that self-initiation occurs when active monomers are used in CGC.

Based on the CGC mechanism proposed in the literature,[1–5] 'deactivated' monomers, that is, monomers where the amine has been deprotonated, are expected to not react with each other. However, the above results demonstrate that this is not true for all systems. A proposed hypothesis for the existence of self-initiation with the activated monomers is the presence of a measurable

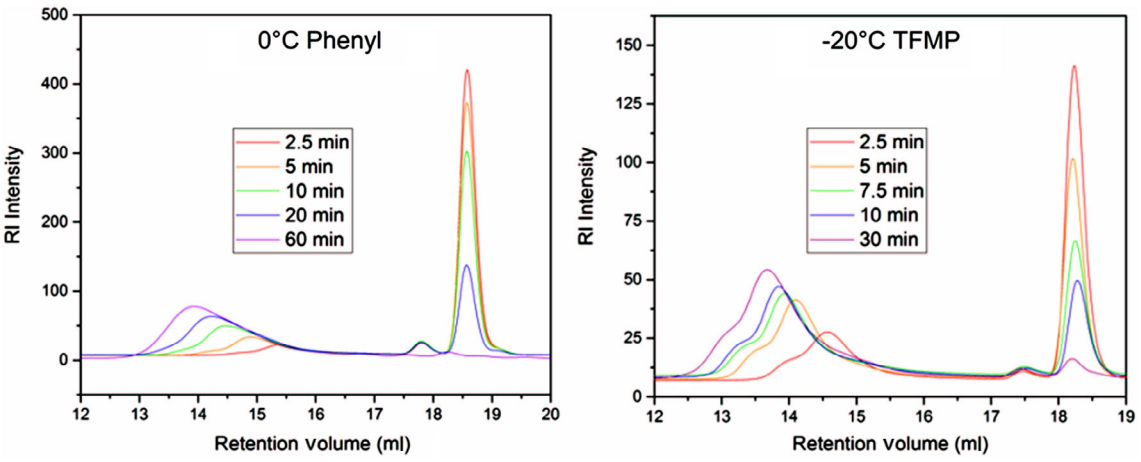

FIGURE 1 Gel-permeation chromatography (GPC) traces displaying the progress of reactions employing no initiators using one equivalent of LiHMDS base for the monomers P-OAB and TFMP-OAB at different temperatures [Color figure can be viewed at wileyonlinelibrary.com]

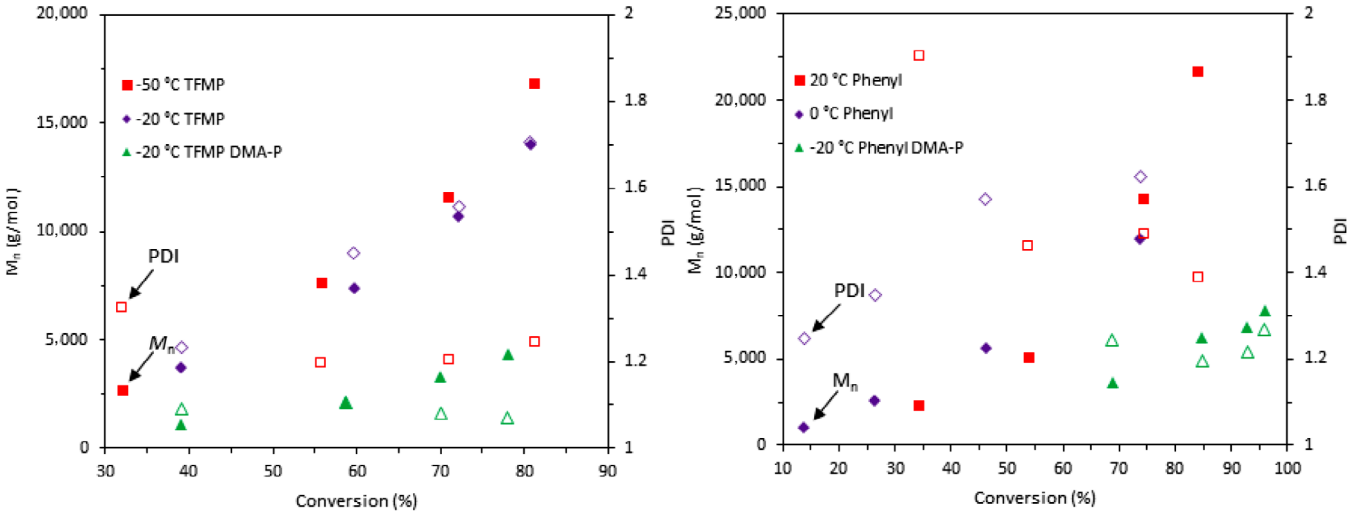

FIGURE 2 Average molecular weight (M_n) and polydispersity index (PDI) evolution with conversion for polymerizations employing no initiator and DMA-P initiators for phenyl and trifluoromethyl (TFMP) monomers at different temperatures [Color figure can be viewed at wileyonlinelibrary.com]

concentration of protonated monomer, when equimolar amounts of base and monomer are used, making self-initiation more probable. This process would be a result of the higher reactivity of the protonated monomer toward nucleophilic attack, due to the lack of the 'deactivating' effect of the negative charge that the deprotonated amine provides. This hypothesis suggests that if all monomer was converted to the deactivated, deprotonated analogues, then self-initiation would either stop or be diminished, due to no protonated monomer in the system.

This was investigated by performing similar polymerizations as previously for TFMP-OAB and P-OAB; however, in each case 10 equivalents of base to monomer was used (Figure 3). The kinetic plots when using 10 equivalents of base demonstrate that the excess base slows the self-initiated polymerization kinetics by almost two orders of magnitude, but it does not completely stop the polymerization from occurring. Whereas, the use of excess base has little effect on the systems where the initiator is used, regardless of the monomer type or temperature. These results show that monomers with more reactive ester groups, such as TFMP-OAB and P-OAB, remain reactive enough toward nucleophilic attack without the presence of initiator and a large excess of base. These observations are important to the field, as in polymerizations to produce high molecular weight polymers, a low concentration of initiator is required. However, as the concentration of initiator with respect to monomer is decreased, the probability of self-initiation influencing the polymerization will increase, resulting in polymers with broader molecular weight distributions and, in the cases of the self-initiated chains, different end groups. Therefore, in order to maintain control over the polymerization it is important to ensure that chain initiation from the externally added initiator dominates over self-initiation.

3.2 | Employing a stronger LDA base

The notion that there may be protonated monomer available for reaction suggests that the LiHMDS base employed for the reactions may not be strong enough to fully deprotonate the monomer, even when the base is in excess.

To examine the effect of base strength on the CGC process, polymerizations of the previous monomers were conducted with LDA as the base. As with LiHMDS, LDA is considered to be a non-nucleophilic base, with the *pKa* of the conjugate acid, diisopropylamine, being 36.[25] This is 6 orders of magnitude less acidic than the conjugate acid of LiHMDS, ($pKa = 30$), demonstrating that LDA is a much stronger base.[26] When examining CGC aromatic polyamide literature for the use of LDA as the base, there are only two previous examples and the results from these papers contradict each other.[10,27] The first paper examines the CGC of M-OAB using LDA as the base, in the presence of an initiator, and reports that LDA is not capable of polymerizing the monomer. The lack of polymerization was attributed to the higher nucleophilicity of LDA, compared to the previously successful LiHMDS, resulting in reaction with the ester end group and terminating the reaction.[10] However, the second paper reported that LDA was successful in the CGC of the meta variation of the methyl ester monomer, methyl 3-(octylamino) benzoate, but without complete conversion.[27] The lower conversion

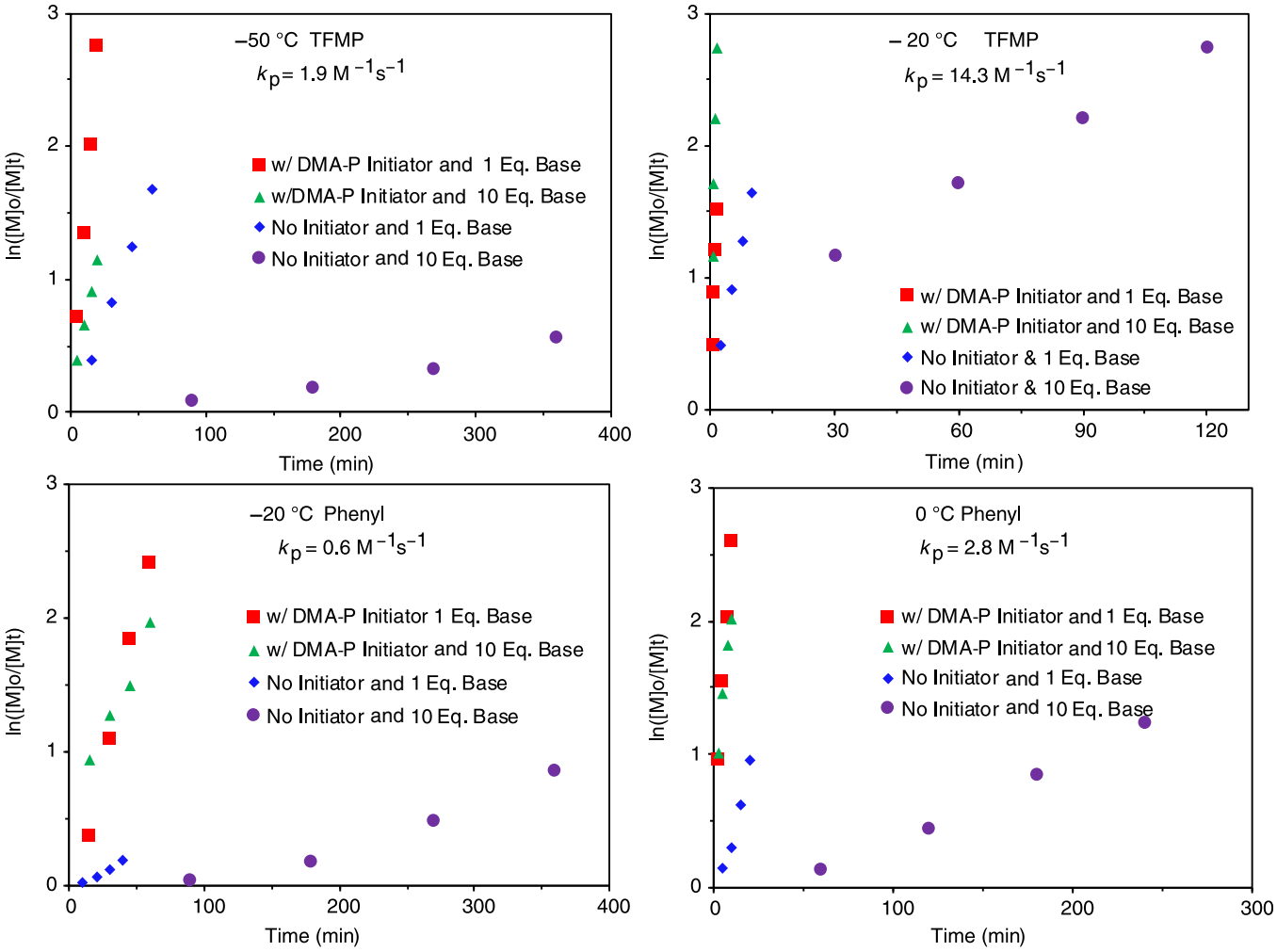

FIGURE 3 Kinetic data relating the use of $[I]_0 = 0.001$ M DMA-P initiator or no initiator with one equivalent and 10 equivalents of base for the polymerization of P-OAB and TFMP-OAB. Propagation rate constants (k_p) are for system with DMA-P initiator and one equivalent of base and calculated by dividing the slope by the initial initiator concentration [Color figure can be viewed at wileyonlinelibrary.com]

TABLE 1 Polymerization results when LDA was employed as the base. Conversion and number average molecular weights (M_n) were calculated using NMR, and the polydispersity indexes (PDIs) was obtained from GPC

Monomer	Conversion (%)	Theoretical M_n (g/mol)	M_n (NMR) (g/mol)	M_n (GPC) (g/mol)	PDI
M-OAB	80	9,200	9,240	5,260	1.08
P-OAB	93	10,700	10,740	10,360	1.11
TFMP-OAB	97	11,150	11,210	13,380	1.16

was attributed to the replacement of the end group with the more nucleophilic LDA base during the course of the polymerization, via a mechanism similar to that reported by Yokozawa in the first paper.[10]

Despite these conflicting results regarding the use of LDA for CGC, polymerizations were conducted using the monomers M-OAB, P-OAB, and TFMP-OAB, and the initiator MP-B with LDA as the base (Scheme S1). To ensure the purity of the LDA it was titrated using diphenyl acetic acid to establish an accurate concentration. A polymerization time of 6 hr was employed for all monomers. The reaction with TFMB-OAB was conducted at −78°C, P-OAB at −20°C, and M-OAB at 20°C, and in each case, polymer was formed. The molecular weight, PDI, and conversions data for the polymerizations is listed in Table 1. The NMR spectra for the

produced polymer in each case resembled that for the polymer made using the LiHMDS base, with no obvious difference in end groups. However, in each case the polymerizations with LDA did not reach 100% conversion, as is usually observed when LiHMDS is used as the base. The lower conversion is also evident from the GPC traces, with a monomer peak appearing at the typical 18.5 ml retention time (see Supporting Information). As can be seen in Table 1, experimental molecular weights very close to theoretical and low PDIs were obtained for each of the polymers suggest that the polymerizations follow the CGC mechanism These results differ from the previous literature examining the CGC of M-OAB with LDA, but tend to agree with results presented in the paper examining the meta monomer.[27] As the NMR spectra of the resulting polymers show the expected methyl ester signal from propagating end of the polymer chain, it appears that LDA does not react with the chain end, as suggested previously.[27] It is unclear what other side reactions LDA may be participating in, especially as the NMR of the polymers mimics those obtained when LiHMDS is used. However, it has been previously shown that LDA can undergo side reactions with small molecule aromatic substrates. For example, reports have shown that an aromatic ring containing an electron-withdrawing carbonyl compound or halogenated substituent can participate in lithiation of the rings in the presence of LDA.[28–33] As each of the monomers used in this study has an ester attached to the aromatic ring, it is possible that side reactions, such as lithiation, is making some of the monomer unreactive to polymerization. As such, even though polymer can be produced with LDA as the base, the presence of side reactions makes it not ideal as the base for CGC polymerizations to produce aromatic polyamides.

3.3 | Effect of initiator structure on polymerization control

As mentioned previously, it is important for any controlled polymerization technique to have quick initiation relative to propagation for the preparation of well-defined polymers with narrow molecular weight distributions. Based on the previous results, it is evident that CGC polymerizations can occur without initiators for more reactive monomers and, while this reaction appears to happen relatively quickly, it can still result in broader molecular weight distributions. As such, an approach to improve the control over the CGC of these monomers would be to design initiators that have improved reactivity. To examine this hypothesis, a series of different initiators were synthesized with varying substituents in the para positions and used to polymerize the more reactive monomers P-OAB and TFMP-OAB (Scheme 3). The initiator structure was varied with substituents of either electron-withdrawing or donating character and the effect of structure on polymerization control was observed by monitoring the molecular weight properties of the polymers produced (Figure 4 and Table 2).

Figure 4 provides GPC traces from the polymerization of both the P-OAB and TFMP-OAB monomers at −20°C, with different initiators and using LiHMDS as the base. In each case, the polymerizations were taken to 100% conversion and the theoretical molecular weight was calculated to be 11,500 g/mol. These results show that the majority of the initiators used provide polymers with relatively low molecular weight distributions when compared to the self-initiated reactions (Figure 4). For each monomer, initiators based on the original DMA-P structure but with electron donating or withdrawing substituents in the para position of the phenoxide-leaving group,

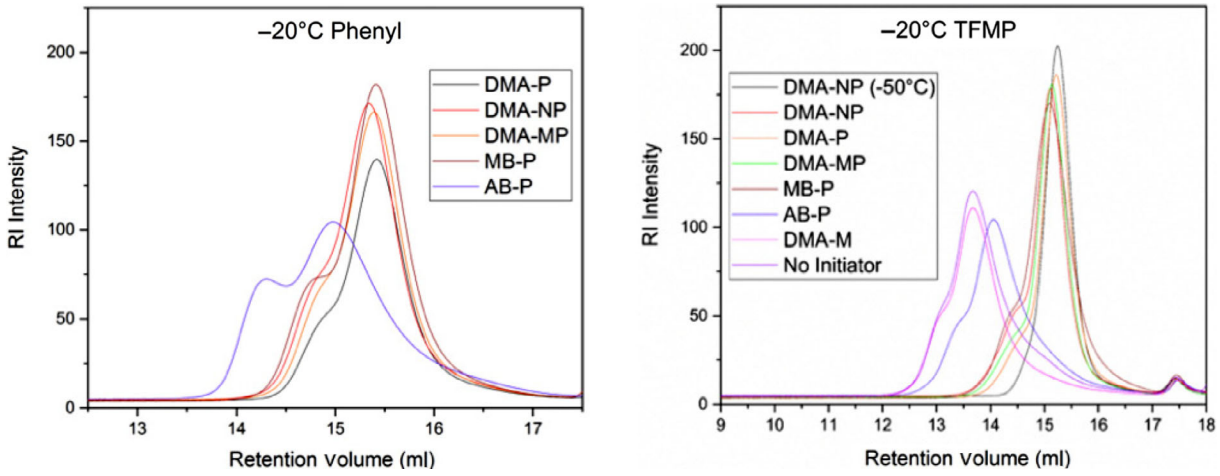

FIGURE 4 Gel-permeation chromatography (GPC) traces resulting from polymers formed using candidate initiators using either P-OAB or TFMP-OAB monomers at −20°C [Color figure can be viewed at wileyonlinelibrary.com]

TABLE 2 Summary of number average molecular weights (M_n) and polydispersity index (PDI) for P-OAB and TFMP-OAB monomers with different initiators at −20°C and 100% conversion

	PDI		M_n (GPC) (g/Mol)	
Initiator molecule	**P-OAB**	**TFMP**	**P-OAB**	**TFMP**
DMA-NP (−50°C)	—	1.08	—	7,390
DMA-NP	1.17	1.20	7,360	9,640
DMA-P	1.16	1.19	6,950	8,700
DMA-MP	1.17	1.27	7,180	8,790
MB-P	1.20	1.27	5,920	9,140
AB-P	1.42	1.67	7,690	19,440
DMA-M	—	1.63	—	30,800
No initiator and one eq. base	—	1.75	—	21,660

Abbreviation: PDI, polydispersity index.

had GPC traces with lower molecular weights and narrower molecular weight distributions when compared to self-initiated systems or systems with deactivated initiators, that is initiators with electron donating groups para to the ester. This is also quantitatively confirmed from PDI and M_n values for these systems (Table 2).

Despite the improved molecular weight control and narrower distributions, the more reactive initiators still produce distributions with small high molecular weight shoulders on the GPC traces (Figure 4). It is proposed that the higher molecular weight shoulders are due to the self-initiation process. When monomers self-initiate, one chain end will have an amine, either in the protonated or deprotonated state. This amine can add to propagating chains via the usual CGC process. Depending on the size of the self-initiated chain, addition of this to another propagating chain will result in multiple monomers added at once, rather than the standard one monomer at a time, resulting in higher molecular weights and broader molecular weight distributions.

The addition of electron-donating groups to the initiators tended to produce higher molecular weight polymers with broader distributions, where self-initiation tended to dominate, as a result of the weakly active initiator. It seems that the inductive effect on the parent benzoate plays a larger role in initiation efficiency than the reactivity of the substituted phenyl ester, due to the broad molecular weight distribution achieved when using AB-P, despite it having the relatively reactive phenyl ester group. The initiator with the methyl ester group, DMA-M, also produced polymer with higher molecular weights and broader molecular weight distributions. This is due to the previously reported poor reactivity of methyl esters toward the CGC process.[8] Both initiators produced polymers that resemble those produced using no initiators for the TFMP monomer suggesting that they are ineffective at starting the polymerization before self-initiation can occur.

No polymer was produced for the P-OAB monomer at −50°C with the DMA-NP initiator, at −20°C with the DMA-M initiator, or at −20°C with no initiator and one equivalent of base. It has been previously shown that the P-OAB monomer does not react at −50°C.[8] In addition, results above show very little self-initiation for the P-OAB monomer at −20°C (Figure 3). As such, all of these results were expected.

3.4 | Computation

In order to help understand the results of these experiments, DFT calculations were carried out on the initiation mechanisms previously discussed. The initiation reaction studied computationally is shown in Scheme 4. In addition, the reaction for self-initiation was also investigated. In both cases, the octyl group on the monomers was replaced with an ethyl chain for simplicity and to limit the computational cost. Calculations were also performed to determine the thermodynamic barriers and the electrophilic nature of the reactive carbonyl group to understand what factors govern the initiation process in both the initiator and self-initiator cases.

3.4.1 | Energetics of varying initiator in CGC mechanism containing initiator

The thermodynamics and kinetics for the reaction of monomer with different initiators was calculated to observe the effect of modifying the initiator structure. In accord with the experimental discussion, the initiator was changed in two ways to determine the effect of modifying the functional groups on the initiator. The initiator was altered at the R-position while keeping R′ as a phenyl group (Scheme 4) to determine the inductive effect of the

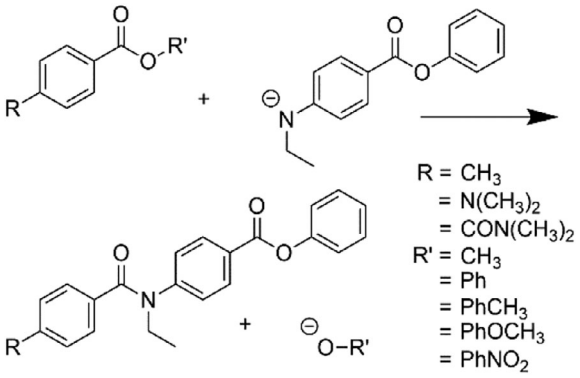

SCHEME 4 Initiation reaction studied computationally to examine the effect of varying initiator structure

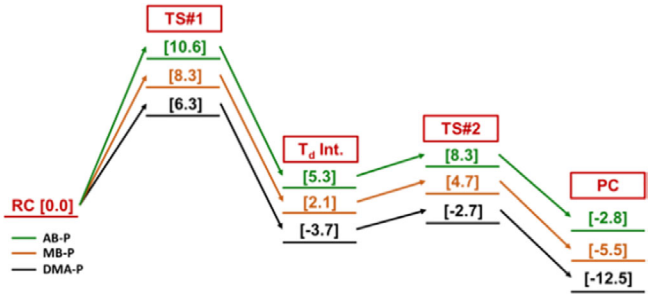

FIGURE 5 Energetics for the initiation mechanism varying the para substituent of the aromatic initiator of a chain-growth condensation (CGC) polymerization calculated using M062X/6–31 + G(d) level of theory. RC, TS#1, Td Int. TS#2, and PC correspond to the reactant complex, the first transition state, the tetrahedral intermediate, the second transition state, and the product complex, respectively. All numbers shown are in kcal/mol [Color figure can be viewed at wileyonlinelibrary.com]

substituent at the para position of the aromatic initiator on the activation energy and electrophilicity of the carbonyl group. Second, the leaving group (R′) was changed while keeping the R-group as DMP to understand the leaving group effects on the activation energy and electrophilicity of the initiation reaction.

The initiators DMA-P, MB-P, and AB-P were examined experimentally to determine if the rate of initiation increases control over the polymerization and reduces the amount of self-initiation during the polymerization. Computational studies of these initiators show the calculated reaction energetics follow the same trend observed experimentally for the reactivity of the initiators. The most reactive initiator was calculated to be DMA-P followed by MB-P and the least reactive initiator was shown to be AB-P (Figure 5). The addition of monomer in the CGC polymerization mechanism goes through two steps: (a) attack of the nucleophile on the ester carbonyl carbon to form the tetrahedral intermediate, and (b) elimination from the tetrahedral intermediate to produce the polymer product with one additional monomer unit and the phenoxide leaving group. The transition states (TS) for both of these steps were calculated. DMA-P was observed to have the lowest TS#1 energy barrier for nucleophilic attack of the carbonyl ester group at 6.3 kcal/mol followed by MB-P (8.3 kcal/mol) and AB-P (10.6 kcal/mol). The energy barrier for nucleophilic attack is primarily dependant on the electrophilicity of the carbonyl group. The electron-withdrawing nature of the dimethyl amide increases the electrophilic nature of the carbonyl, whereas the electron donating dimethyl amine lowers the electrophilicity resulting in a higher energy barrier for nucleophilic attack.

Upon nucleophilic attack, the initiator and reactive monomer form the tetrahedral intermediate. As with nucleophilic attack, the stabilization of the intermediate is also dependent on the nature of the functional group. The intermediate formed for DMA-P is much more stabilized, at −3.7 kcal/mol, than MB-P and AB-P (2.1 and 5.3 kcal/mol, respectively) and is the only exothermic reaction when forming the tetrahedral intermediate. This is due to the electron-withdrawing nature of the dimethyl amide group. The slowest reacting initiator was AB-P, which contains the donating group dimethyl amine. After the formation of the tetrahedral intermediate, the energy barriers for the decomposition to form the propagating chain and phenoxide leaving group for all three initiators are approximately the same. This is expected as the para substituent would only affect the formation of the tetrahedral intermediate not the decomposition.

The various initiator leaving groups under investigation are shown in Scheme 1 and were studied with the DMA initiator. Figure 6 shows the initiation energetics for the five leaving groups studied. As previously demonstrated,[8] phenoxide leaving groups have a lower activation barrier than alkoxide leaving groups due to the increased electrophilicity of the carbonyl group and delocalization of the charge stabilizing both the tetrahedral intermediate and the leaving group.

This was also observed for the initiators in this study as the methoxy leaving group has a large activation barrier, 8.4 kcal/mol, for nucleophilic attack and an even larger activation barrier, 19.6 kcal/mol, for the decomposition of the intermediate and formation of the methoxide-leaving group. For the phenyl-based initiators, the leaving groups with electron-withdrawing groups on the aromatic ring have the lowest energy barriers (4.5 kcal/mol for both Ph-CF_3 and Ph-NO_2) for nucleophilic attack and are the most exothermic when forming the tetrahedral intermediate. Electron-donating groups have the highest activation barriers (9.1 kcal/mol for Ph-

OMe) for TS#1 and form the least stable tetrahedral intermediate. This trend is due to the ability of the electron-withdrawing group to pull more charge away from the carbonyl carbon and into the ring, stabilizing the formation of the tetrahedral intermediate and elimination to produce the phenoxide-leaving group. Whereas, electron-donating groups stabilize the carbon on the carbonyl group more than alkyl-leaving groups but not as efficiently as electron-withdrawing groups. The energetics for Ph-OMe leaving group do not follow the trend discussed for TS#1 because no diffuse function was used in the computational method. This results in the energies to be overestimated for Ph-OMe for the initiation mechanism.

3.4.2 | Charges reflecting electrophilicity of the initiator carbonyl

In an attempt to further understand the behavior observed in the experimental results above, partial atomic charges were calculated to examine the electrophilic nature of the initiators carbonyl group participating in the CGC reaction. When examining the electrophilicity of the initiators, the trend observed was that the most reactive initiator has the most electrophilic ester carbonyl group as shown in Table 3. The more electron-withdrawing dimethyl amide group in DMA-P has the most positive charge on the carbon and least negative charge on the neighboring oxygens of the carbonyl group, while the dimethylamino group (AB-P) has the lowest positive charge on the carbon and highest negative charge on the two oxygen, with the neutral methyl group in the middle. These results show that the nature of the functional group on the initiator can increase or decrease the electrophilicity of the ester carbonyl group resulting in the observed trends in reaction energetics previously discussed.

When examining the substituent effect of the ester-leaving group of the initiators, there is a similar trend observed. In the case of the DMA-based initiators, the substituent on the ester affects the electrophilicity of the reactive carbonyl carbon (Table 4). The methoxy-leaving group (DMA-M) was found to have the lowest positive charge on the carbon and highest negative charge on the oxygen atoms making this carbonyl unit the least overall electrophilic. All the phenyl-based leaving groups contain a lower amount of overall charge on the carbonyl group due to charge delocalization into the ring. The most electrophilic carbonyl group contains the phenyl-leaving group with a strong withdrawing group para to the ester (DMA-NP). These results are in accord with the previously discussed reaction energetics where DMA-NP had the lowest energy barriers and DMA-M had the highest energy barriers for nucleophilic attack on the initiator.

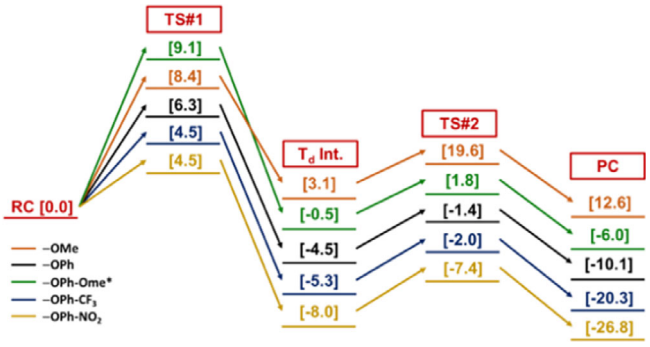

FIGURE 6 Energetics for varying the ester-leaving group of the DMA initiator for the initiation mechanism of a chain-growth condensation (CGC) polymerization calculated using M062X/6–31 + G(d) level of theory. RC, TS#1, Td Int. TS#2, and PC correspond to the reactant complex, the first transition state, the tetrahedral intermediate, the second transition state, and the product complex, respectively. All numbers shown are in kcal/mol [Color figure can be viewed at wileyonlinelibrary.com]

3.4.3 | Charges and energetics reflecting electrophilicity of protonated and deprotonated monomer and dimer

Calculations were also performed on the self-initiation mechanism to help understand the reactivity of the various species present when forming the active initiator through the self-condensation mechanism. To do this, the energetics to form dimers and the partial atomic charges of the carbonyl group of the dimers were calculated for four different species that may exist throughout the

TABLE 3 Partial atomic charges of reactive carbonyl atoms of three initiators with phenyl ester and varying functional group

Atom (in bold)	DMA-P	MB-P	AB-P
O═C—**O**R	−0.563	−0.566	−0.572
O═**C**—OR	0.850	0.848	0.844
O═C—OR	−0.616	−0.624	−0.641

TABLE 4 Charge of reactive carbonyl atoms for initiators with various ester-leaving groups and the dimethyl amide substituent

Atom (in bold)	DMA-M	DMA-P	DMA-MP	DMA-NP
O═C—**O**R	−0.569	−0.563	−0.562	−0.560
O═**C**—OR	0.845	0.848	0.849	0.850
O═C—OR	−0.640	−0.616	−0.615	−0.605

polymerization that would lead to polymer growth (Figure 7). The energetics of the deprotonated monomer attacking another deprotonated monomer and the energetics of the deprotonated monomer attacking a protonated monomer were both calculated to observe if, thermodynamically, the formation of dimers is feasible during the initiation process. The calculations show that the activation barrier for forming either dimer is larger than the initiation process when initiator is present (Table 5). However, the formation of dimer with a protonated monomer is low enough (46.8 kJ/mol, Table 5) that it could potentially occur during the reaction. This is in agreement with experimental observations, as it was shown that with the addition of an initiator the rate of polymerization is faster than without initiator. The dimer produced with deprotonated monomer was calculated to have a very large energy barrier (75.8 kJ/mol, Table 5) leading to the conclusion that the mechanism was unlikely to occur.

The calculated E_a values also help explain the experimental results observed in Figure 4. Experimentally for polymerization of the TFMP-OAB monomer at −20°C, significantly higher molecular weights and broader molecular weight distributions were observed for the AB-P and DMA-M initiators and when no initiator was used. The GPC traces for polymer produced with the DMA-M initiator and with no initiator for this system were almost identical, while the trace for the AB-P initiator was shifted to slightly lower molecular weight (Figure 4). Table 5 indicates the E_a value for the DMA-M initiator is over 20 kJ/mol higher than for the protonated dimer. This suggests that self-initiation should dominate in this system, which is confirmed by the similar GPC trace to the case with no initiator. Whereas, the E_a for the AB-P initiator is of a similar magnitude to the protonated dimer, indicating a balance between conventional and self-initiation should occur and results in a GPC trace with a molecular weight closer to theoretical but still with a broad molecular weight distribution. All of the other initiators used have E_a values at least 12 kJ/mol lower than the protonated monomer and their molecular weight values are very close to theoretical and all have PDI values less than 1.3, indicating a well-controlled CGC process.

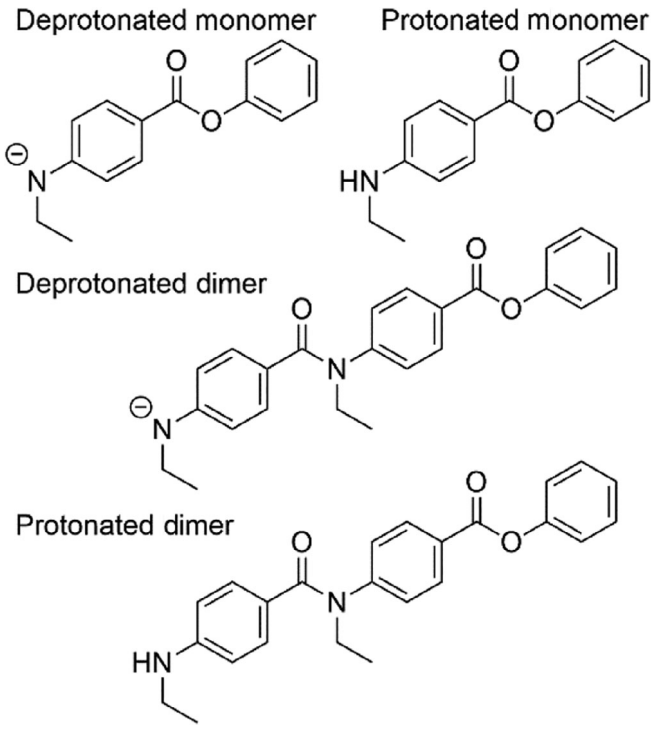

FIGURE 7 Structures used to calculate partial atomic charges on the atoms included in the ester carbonyl group for the three monomers investigated

As discussed previously, the deprotonated and protonated versions of the monomer were hypothesized to exist in the solution and lead to self-initiation mechanism. To understand the electrophilicity of the four species discussed, the partial atomic charges of the ester carbonyl group were calculated (see Table S1). These results suggest that there is a difference between the charge on the carbonyl for protonated and deprotonated monomer, with a more positive charge on the carbonyl carbon for the protonated monomer. For the deprotonated monomers, some of the charge for the nucleophilic nitrogen delocalizes through the ring and onto the carbonyl group, which lowers the electrophilicity of the carbonyl carbon. This process is typically discussed in literature as the deactivation process for the carbonyl on the reactive monomer.[1–5] A more electrophilic carbonyl carbon, by conventional CGC theory, such as that for the protonated monomer, means that it is more reactive and is a possible source for dimer

TABLE 5 Computational activation energies for the various initiators investigated in this study

Initiator	Computational E_a (kJ/Mol)
Deprotonated dimer	75.8
DMA-M	68.8
Protonated dimer	46.8
AB-P	44.4
MB-P	34.6
DMA-MP	33.2
DMA-P	26.5
DMA-NP	18.8
DMA-TFMP	18.7

Note: E_a values were calculated for rate limiting step.

formation. These results confirm our previous hypothesis that dimer formation between deprotonated monomer and protonated monomer may be responsible for self-initiation.

Next, the partial atomic charges were calculated for atoms of the carbonyl for the two potential versions, protonated and deprotonated, of the dimer formed by the coupling of two monomers (see Table S2). The results show that there is very little difference in charge on the carbon of the carbonyl group. The charge on the carbon atom of the carbonyl group for both of the dimer structures is more positive than both versions of the monomer structures and is similar to the charges of the carbonyl unit of the DMP initiators. This suggests that if a dimer is formed in solution, it could take over the role as an initiator. It is believed that once the dimer forms, due to the electrophilicity of the carbonyl on the ester-leaving group, the polymerization can be effectively initiated.

4 | CONCLUSIONS

Recent studies have demonstrated that reactivity of aminobenzoate monomers depends on the nature of the ester substituent greatly when employed in a CGC polymerization. More reactive monomers contain electron-withdrawing substituents on the esters that result in more stable leaving groups. The increased reactivity of these esters posed interesting challenges, due to the possibility of the monomers to undergo self-initiation and polymerize with no initiator present. The challenge addressed here was to understand the self-initiation behavior and find initiators that allow for control to be achieved. Results demonstrate that the relative amount of LiHMDS base can be used to slow, but not stop, the self-initiation reaction for monomers that experience this reaction. LDA, being a stronger base works for the polymerization, producing polymers with narrow distributions, but is not a good choice, due to the high strength of the base resulting in incomplete conversion of monomer. Enhanced control over the polymerization was achieved by using the most reactive initiators, which have electron-withdrawing substituents both on the benzoate backbone and the leaving group of the ester.

Computational results reinforce the conclusions derived from the experimental investigation. The calculated reaction energetics match experimental findings, where the initiators based on DMA were the most reactive. The initiators containing electron-withdrawing phenoxide leaving groups have the lowest activation barrier. The more reactive initiators help in the reduction of self-initiation and provide more control over the polymerization. The computational findings for the self-initiation mechanism show that a reaction between protonated and deprotonated monomer is a potential source of the experimentally observed self-initiation.

From these studies, it has been demonstrated that balancing the relative rates of initiation, propagation, and self-initiation is key when attempting to use more reactive esters to produce well-defined aromatic polyamides via the CGC process.

ACKNOWLEDGMENTS

S. G. B. and C. J. R. gratefully acknowledges the support of this work by the National Science Foundation under grant CHE MSN #1807863 and S. G. B., D. P., and A. T. also acknowledge support by the National Science Foundation under grant ENG # 1460712. B. D. E. and S. V. gratefully acknowledge the computational resources from high performance computing facility at CSM.

ORCID

Stephen G. Boyes https://orcid.org/0000-0003-4821-2785

REFERENCES

[1] T. Yokozawa, Y. Ohta, *Chem. Commun.* **2013**, *49*, 8281.
[2] T. Yokozawa, Y. Ohta, *Chem. Rev.* **2016**, *116*, 1950.
[3] T. Yokozawa, A. Yokoyama, *Chem. Rev.* **2009**, *109*, 5595.
[4] T. Yokozawa, A. Yokoyama, *Chem. Rec.* **2005**, *5*, 47.
[5] A. Yokoyama, T. Yokozawa, *Macromolecules* **2007**, *40*, 4093.
[6] T. Yokozawa, A. Yokoyama, *Prog. Polym. Sci.* **2007**, *32*, 147.
[7] W. A. Braunecker, K. Matyjaszewski, *Prog. Polym. Sci.* **2007**, *32*, 93.
[8] F. C. Prehn Jr., B. D. Etz, S. Vyas, S. G. Boyes, *J. Polym. Sci. Part A Polym. Chem* **2020**. https://doi.org/10.1002/pol.20200435.
[9] T. Yokozawa, R. Sugi, T. Asai, A. Yokoyama, *Chem. Lett.* **2004**, *33*, 272.
[10] T. Yokozawa, D. Muroya, R. Sugi, A. Yokoyama, *Macromol. Rapid Commun.* **2005**, *26*, 979.
[11] Frisch, M. J., Trucks, G. W., Schlegel, H. B., Scuseria, G. E., Robb, M. A., Cheeseman, J. R., Scalmani, G., Barone, V., Mennucci, B., Petersson, G. A., Nakatsuji, H., Caricato, M., Li, X., Hratchian, H. P., Izmaylov, A. F., Bloino, J., Zheng, G., Sonnenberg, J. L., Hada, M., Ehara, M., Toyota, K., Fukuda, R., Hasegawa, J., Ishida, M., Nakajima, T., Honda, Y., Kitao, O., Nakai, H., Vreven, T., Montgomery, J. A., Jr., J. E. P., Ogliaro, F., Bearpark, M., Heyd, J. J., Brothers, E., Kudin, K. N., Staroverov, V. N., Kobayashi, R., Normand, J., Raghavachari, K., Rendell, A., Burant, J. C., Iyengar, S. S., Tomasi, J., Cossi, M., Rega, N., Millam, J. M., Klene, M., Knox, J. E., Cross, J. B., Bakken, V., Adamo, C., Jaramillo, J., Gomperts, R., Stratmann, R. E., Yazyev, O., Austin, A. J., Cammi, R., Pomelli, C., Ochterski, J. W., Martin, R. L., Morokuma, K., Zakrzewski, V. G., Voth, G. A., Salvador, P., Dannenberg, J. J., Dapprich, S., Daniels, A. D., Farkas, Ö., Foresman, J. B., Ortiz, J. V., Cioslowski, J., Fox, D. J. Gaussian, Inc., Wallingford CT, **2016**. https://gaussian.com/citation/
[12] Y. Zhao, D. G. Truhlar, *Theor. Chem. Acc.* **2008**, *120*, 215.
[13] W. J. Hehre, K. Ditchfield, J. A. Pople, *J. Chem. Phys.* **1972**, *56*, 2257.

[14] P. C. Hariharan, J. A. Pople, *Theor. Chim. Acta* **1973**, *28*, 213.
[15] J. P. Foster, F. Weinhold, *J. Am. Chem. Soc.* **1980**, *102*, 7211.
[16] V. Barone, M. Cossi, J. Tomasi, *J. Comput. Chem.* **1998**, *19*, 404.
[17] S. Canneaux, F. Bohr, E. Henon, *J. Comput. Chem.* **2014**, *35*, 82.
[18] K. Yoshino, A. Yokoyama, T. Yokozawa, *J. Polym. Sci. Part A Polym. Chem.* **2009**, *47*, 6328.
[19] Y. Ohta, M. Karasawa, T. Niiyama, A. Yokoyama, T. Yokozawa, *J. Polym. Sci. Part A Polym. Chem.* **2014**, *52*, 360.
[20] F. C. Prehn, S. G. Boyes, *Macromolecules* **2015**, *48*, 4269.
[21] R. Sugi, A. Yokoyama, T. Furuyama, M. Uchiyama, T. Yokozawa, *J. Am. Chem. Soc.* **2005**, *127*, 10172.
[22] T. Ohishi, R. Sugi, A. Yokoyama, T. Yokozawa, *Macromolecules* **2008**, *41*, 9683.
[23] K. Yoshino, A. Yokoyama, T. Yokozawa, *J. Polym. Sci. Part A Polym. Chem.* **2011**, *49*, 986.
[24] R. Sugi, D. Tate, T. Yokozawa, *J. Polym. Sci. Part A Polym. Chem.* **2013**, *51*, 2725.
[25] R. R. Fraser, M. Bresse, T. S. Mansour, *J. Am. Chem. Soc.* **1983**, *105*, 7790.
[26] R. R. Fraser, T. S. Mansour, *J. Org. Chem.* **1984**, *49*, 3442.
[27] T. Ohishi, R. Sugi, A. Yokoyama, T. Yokozawa, *J. Polym. Sci. Part A Polym. Chem.* **2006**, *44*, 4990.
[28] P. Beak, V. Snieckus, *Acc. Chem. Res.* **1982**, *15*, 306.
[29] S. Caron, J. M. Hawkins, *J. Org. Chem.* **1998**, *63*, 2054.
[30] B. Bennetau, J. Mortier, J. Moyroud, J.-L. Guesnet, *J. Chem. Soc. Perkin Trans. 1*. **1995**, *10*, 1265.
[31] T. L. Rathman, W. F. Bailey, *Org. Process Res. Dev.* **2009**, *13*, 144.
[32] H. Pellissier, M. Santelli, *Tetrahedron* **2003**, *59*, 701.
[33] F. Gohier, J. Mortier, *J. Org. Chem.* **2003**, *68*, 2030.

SUPPORTING INFORMATION

Additional supporting information may be found online in the Supporting Information section at the end of this article.

How to cite this article: Prehn FC Jr, Etz BD, Price D, et al. Chain-growth polycondensation via the substituent effect: Investigation in to the role of initiator and base on the synthesis of poly(*N*-octyl benzamide). *J Polym Sci*. 2020;58:2407–2422. https://doi.org/10.1002/pol.20200436